



TITLE:

Vacancies selectively induced and specifically detected on the two sublattices of the intermetallic compound MoSi₂

AUTHOR(S):

Zhang, XY; Sprengel, W; Blaurock, K; Rempel, AA;
Reichle, KJ; Reimann, K; Inui, H; Schaefer, HE

CITATION:

Zhang, XY ...[et al]. Vacancies selectively induced and specifically detected on the two sublattices of the intermetallic compound MoSi₂. PHYSICAL REVIEW B 2002, 66(14): 144105.

ISSUE DATE:

2002-10-01

URL:

<http://hdl.handle.net/2433/50077>

RIGHT:

Copyright 2002 American Physical Society

Vacancies selectively induced and specifically detected on the two sublattices of the intermetallic compound MoSi₂

X. Y. Zhang,^{1,2,*} W. Sprengel,² K. Blaurock,² A. A. Rempel,^{2,3} K. J. Reichle,² K. Reimann,² H. Inui,⁴ and H.-E. Schaefer²

¹College of Materials Science and Engineering, Yanshan University, 066004 Qinhuangdao, People's Republic of China

²Institut für Theoretische und Angewandte Physik, Stuttgart University, D-70550 Stuttgart, Germany

³Institute of Solid State Chemistry, Russian Academy of Sciences, Ekaterinburg, Russia

⁴Department of Materials Science and Engineering, Kyoto University, Kyoto, Japan

(Received 1 November 2001; revised manuscript received 12 February 2002; published 11 October 2002)

In the present study vacancies were selectively induced on the Si or predominantly on the Mo sublattices of MoSi₂ single crystals by low-temperature irradiation with electrons of low or high energies. These vacancies were specifically detected by employing two-detector Doppler broadening measurements of the positron-electron annihilation γ quanta in addition to positron lifetime studies. Positron lifetime studies show that two kinds of vacancies on either the Si or the Mo sublattices were induced in MoSi₂ by 0.5- or 3-MeV electron irradiation. After 0.5-MeV electron irradiation Doppler broadening spectra characteristic for Mo are detected, which shows that the vacancies with the 139 ps positron lifetime are located on the Si sublattice. After 3-MeV electron irradiation, only Si atoms were detected to surround the vacancy with the 156 ps positron lifetime, which demonstrates that in this case positrons are predominantly trapped by vacancies on the Mo sublattice. In the present experiment the selective introduction of vacancies and the detection of their location on different sublattices have proven to be a promising technique for specifically studying atomic defects in solids with a complex structure.

DOI: 10.1103/PhysRevB.66.144105

PACS number(s): 61.72.Ji, 71.20.Lp, 61.72.Dd

I. INTRODUCTION

The intermetallic compound MoSi₂ is a promising material for high-temperature structural applications due to its high melting temperature ($T_m = 2293$ K), low mass density, excellent oxidation resistance, and high thermal conductivity.^{1,2} For intermetallic compounds, the high-temperature mechanical properties such as mechanical creep and plasticity are significantly affected by thermal defects such as vacancies.^{3,4} Thermal defects and atomic processes in intermetallic compounds can be studied specifically by positron annihilation spectroscopy⁵ or time-differential length change measurements.⁶ For a detailed understanding of the high-temperature atomic processes in ordered binary intermetallics and more complex solids, it is of interest to selectively induce atomic defects and identify the defects, e.g., vacancies, on the various sublattices. For this type of investigations a combination of positron lifetime spectroscopy and coincident measurements of the Doppler broadened two annihilation photons up to high energies, i.e., high electron momenta can be specifically employed. By the coincident Doppler broadening technique,^{7,8} the studies of the core electron momenta in the vicinity of a vacancy can be used for a local chemical analysis of the atoms surrounding the vacancy. From these data, information can be deduced on the sublattice on which the vacancy is located in an ordered solid compound.

Low-temperature electron irradiation is particularly suitable for a selective introduction of atomic defects as vacancies in the MoSi₂ intermetallic compound due to the considerable mass difference of the Si and Mo atoms, which makes it possible that, during an electron irradiation process, the energy transferred to the lattice atoms suffices for Si dis-

placement but not for that of Mo atoms. As a result, by an appropriate electron energy, e.g., 0.5 MeV, atomic vacancies can be selectively induced on, e.g., the Si sublattice of MoSi₂.

In the present work vacancies are selectively introduced on either of the two sublattices of MoSi₂ and specifically detected by positron annihilation spectroscopy. This type of study is expected to be of interest for the study of atomic defects in complex solids.

II. EXPERIMENTAL PROCEDURE

A master ingot of MoSi₂ was prepared by comelting Mo (99.95%) and Si (99.9999%) in a plasma-arc furnace under an argon atmosphere. The MoSi₂ single crystal was grown using an optical floating-zone furnace at a growth rate of 10 mm/h under Ar gas flow.⁹ The specimens with a size of $8 \times 6 \times 1$ mm³ were cut from the as-grown single crystal by employing a spark erosion technique. They were then polished mechanically and annealed at 800 K for 16 h under vacuum ($p < 10^{-5}$ Pa).

The irradiation of the specimens with electrons of energies between 0.5 and 3 MeV and doses of $3.7 \times 10^{22}/\text{m}^2$ to $7.5 \times 10^{23}/\text{m}^2$ was carried out at low temperatures between 80 and 200 K at the DYNAMITRON accelerator of Stuttgart University, Germany, where electrons with a wide energy range of 0.5 to 4.0 MeV and a fluence of ≈ 0.1 – 0.15 A/m² are available.

The positron lifetime spectra of the annealed or irradiated MoSi₂ specimens were measured at room temperature by a fast-slow $\gamma\gamma$ spectrometer with a time resolution of 210–220 ps (full width at half maximum) using a sandwiched ²²NaCl positron source. The positron lifetimes τ_i and the relative intensities I_i were numerically determined by means of stan-

TABLE I. Positron lifetime components τ_i with their relative intensities I_i ($i=0,1$), the lifetime for positrons in the free state (τ_f) and the vacancy-trapped state (τ_v) as well as the mean positron lifetime $\bar{\tau}$ in the annealed MoSi₂ single crystals before and after electron irradiation with different energies.

Specimen	e^- dose (e^-/m^2)	Number of components	τ_0 (ps)	I_0 (%)	τ_l (ps) ($\tau_l = \tau_v$)	I_l (%)	τ_f (ps)	$\bar{\tau}$ (ps)
Annealed MoSi ₂ (800 K, 16 h)		1	117 ± 1	100	0	0	117 ± 1	117 ± 1
0.5 MeV	7.5 × 10 ²³	2	74 ± 5	28 ± 4	139 ± 2	72 ± 4	113 ± 8	122 ± 2
1 MeV	1.4 × 10 ²³	2	76 ± 3	25 ± 2	156 ± 1	75 ± 1	123 ± 2	136 ± 2
2 MeV	4.4 × 10 ²²	2	58 ± 5	6 ± 1	156 ± 1	94 ± 1		150 ± 2
3 MeV	3.7 × 10 ²²	1	0	0	156 ± 1	100		156 ± 1

dard techniques¹⁰ from positron lifetime spectra with more than 10⁶ total coincidence counts.

The measurements of the Doppler broadening of the positron-electron annihilation γ spectra up to the high momenta of the chemically characteristic core electrons were carried out at room temperature, by measurements of the two annihilation photons with the energies E_1 and E_2 coincidentally, by means of two high-resolution Ge detectors. The high peak-to-background ratio of $>5 \times 10^5$ was achieved by diagonal cuts of the E_1 - E_2 -Doppler spectra along the $E_1 + E_2 = (1022 \pm 1.5)$ keV energy line. Each of these spectra contains more than 4×10^7 coincidence counts for achieving good statistics in the core electron region above $\Delta E = 5$ keV, which corresponds to $p_L \geq 20 \times 10^{-3} m_0 c$ for the core electron momenta. For emphasizing the high-momentum tails, the Doppler spectra measured on MoSi₂, Mo, and Si were normalized to the smoothed Si Doppler spectrum (see Fig. 3) so that the Si spectrum is represented by a straight horizontal line. The reference specimens, a Si single crystal with a [100] direction perpendicular to the surface and a Mo polycrystal, were well annealed at 873 K for 48 h before measurement.

III. RESULTS AND DISCUSSION

Table I exhibits the analysis of the positron lifetime spectra of annealed and irradiated MoSi₂. Only one component with a lifetime of $\tau_0 = (117 \pm 1)$ ps was determined from the lifetime spectrum of annealed MoSi₂, which is similar to the results of (115 ± 2) ps reported by Matsuda, Shirai, and Yamaguchi.¹¹ According to the experimentally deduced dependence of the positron lifetimes in the delocalized free state (τ_f) and in the vacancy-trapped state (τ_v) from the bulk valence electron density in pure metals and compounds in Fig. 1, the positron lifetime of 117 ps measured in annealed MoSi₂ indicates that the MoSi₂ is in the defect-free state without positron trapping at structural vacancies. The dislocation density in the MoSi₂ single crystals is about 10^9 m^{-2} . This yields a separation of dislocations of $30 \times 10^{-6} \text{ m}$, which is much longer than the positron diffusion length (10^{-7} m) and therefore the positron annihilation at dislocations is negligible.

The mean positron lifetime $\bar{\tau}$ of MoSi₂ increases from 117 to 156 ps as the electron irradiation energy increases to 3

MeV (Table I), indicating that vacancies are induced in MoSi₂ by electron irradiation. After irradiation with 0.5-MeV electrons the positron lifetime spectrum of MoSi₂ can be fitted by two lifetime components, one with a long lifetime of (139 ± 2) ps and the other with a short one, from which the lifetime of positron annihilation in the defect-free state can be determined to $\tau_f = (113 \pm 8)$ ps according to the simple two-state trapping model. This is in reasonable agreement with that in annealed MoSi₂ (117 ± 1) ps. Obviously, the long lifetime of 139 ps results from positron annihilation in radiation-induced vacancies. This lifetime, which is relatively low for positron annihilation in a vacancy-trapped state (see Fig. 1), indicates that the positrons are not strongly trapped in the radiation-induced vacancies. As the irradiation energy increases to 3 MeV, a longer lifetime of $\tau_v = 156$ ps appears, which indicates stronger localization of positrons in the vacancies. The significant difference between these positron lifetimes indicates that 0.5-or 3-MeV irradiation gives rise to positron trapping in different types of vacancies.

For a further discussion on which sublattice of MoSi₂

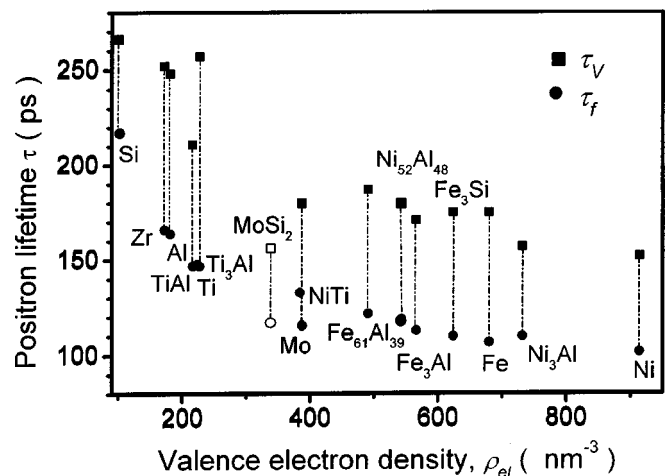


FIG. 1. Relationship between the positron lifetime in the free state (τ_f) and vacancy-trapped state (τ_v) measured by experiment (Refs. 10 and 34) and the valence electron density (ρ_{el}) for pure metals and intermetallic compounds. The valence electron density $\rho_{el} = (n \times N_{el})/V$ is given by the number of atoms (n), the mean number N_{el} of the outer s , p , or d electrons per atom, and the volume of the unit cell (V).

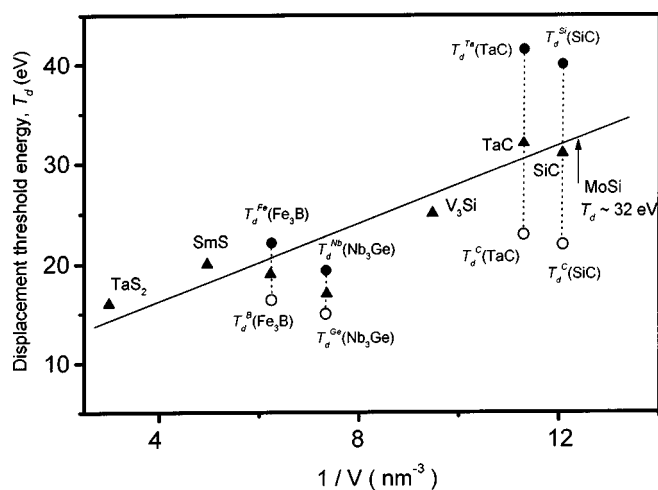


FIG. 2. Relationship between the displacement threshold energies T_d of some compounds (Refs. 12–19) and the reciprocal of their unit-cell volumes V^{-1} . \blacktriangle , mean values; \bullet , heavier atom; \circ , light atom. The position for MoSi is indicated by an arrow.

vacancies are predominantly introduced by low- or high-energy electron irradiation, the threshold displacement energies T_d for the two types of atoms have to be considered. If the energy E^{col} transferred to a lattice atom by an impacting electron is above the T_d , then a permanent atomic displacement is effectuated. Since experimental values for the displacement threshold energies of Si or Mo in MoSi₂, T_d^{Si} and T_d^{Mo} , are unavailable, we will try to make an estimate. Corbett and Bourgoïn reported a linear relationship between the displacement threshold energies and the reciprocal lattice constants for binary compound semiconductors with cubic structures,¹² which has been successfully used to estimate the displacement threshold energy T_d of various compounds.^{13,14} For the estimate of T_d^{Si} and T_d^{Mo} for MoSi₂ a plot of the atomic displacement threshold energies of the components for various compounds as a function of the reciprocal unit-cell volumes (V) is presented in Fig. 2. For MoSi₂ with $1/V = 12.41 \text{ nm}^{-3}$ the displacement threshold energies $T_d^{\text{Si}} = 20\text{--}32 \text{ eV}$ for a Si atom and $T_d^{\text{Mo}} = 32\text{--}40 \text{ eV}$ for a Mo atom in MoSi₂ are estimated from Fig. 2, taking additionally into consideration the slightly lower T_d values for the lighter atom and slightly higher values for the heavier atom as observed, e.g., in TaC and SiC (Fig. 2).

When we now consider the maximum energies transferred

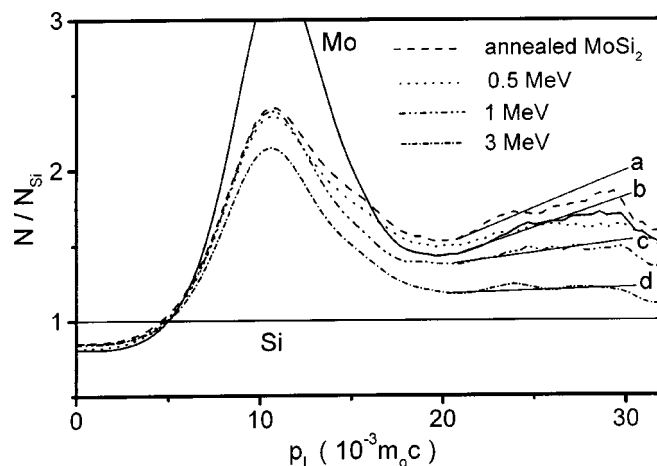


FIG. 3. Ratio of area-normalized counts of two-detector Doppler broadened spectra of positron annihilation in pure Mo, Si and annealed MoSi before and after electron irradiation with different energies at temperatures between 80 and 200 K. The spectra are normalized to the smoothed Si spectrum, which therefore gives a straight line.

to Si atoms ($E^{\text{col}} = 58 \text{ eV}$) or Mo atoms ($E^{\text{col}} = 17 \text{ eV}$) in the case of 0.5-MeV electron irradiation (see Table II), it is evident that only Si atoms but no Mo atoms can be displaced, irrespective of the uncertainties in the estimates of the displacement threshold energies T_d . Therefore, the positron lifetime of $\tau_v = 139 \text{ ps}$ measured after 0.5-MeV electron irradiation can be assigned to positron annihilation exclusively in the vacancies on the Si sublattice, V_{Si} . Then, the lifetime, $\tau_v = 156 \text{ ps}$ after electron irradiation with 3 MeV, is attributed to positron annihilation in the vacancies V_{Mo} on the Mo sublattice, which is further confirmed by the Doppler broadening measurements (see Fig. 3). It should be commented here that both positron lifetimes, for V_{Si} and V_{Mo} , appear to be small compared to the behavior in other solids. This may be due to an only weak positron trapping potential of V_{Si} or a strong structural relaxation of Si atoms around V_{Mo} .

For a specific identification of the location of vacancies in compound solids, the technique of the coincident measurement of the Doppler broadening of the positron-electron annihilation photons has been employed on ZnS_xSe_{1-x},⁸ InP,²⁰ GaAs,²¹ SiC,²² and FeAl,²³ and atomic aggregations in Fe-Cu alloys.²⁴ Positron annihilation with core electrons of high momenta yields larger Doppler shifts of the annihilation photons compared to valence electrons. Therefore, the tail

TABLE II. Maximum energies transferred to a Si or a Mo atom (E^{col}) [$E^{\text{col}} = 2E(E + 2mc^2)/Mc^2$, where E is the energy of the irradiation electrons, c is the velocity of light, m is the rest mass of the electron, and M is the mass of the target atom.] after an elastic collision with electrons of the energies 0.5–3 MeV together with atomic displacement threshold energies (T_d) in MoSi₂.

Atoms	Maximum transferred energies, E^{col} (eV)				Displacement threshold energies in MoSi ₂ , T_d (eV)
	0.5 MeV	1 MeV	2 MeV	3 MeV	
Si	58	155	462	922	20–32
Mo	17	45	135	270	32–40

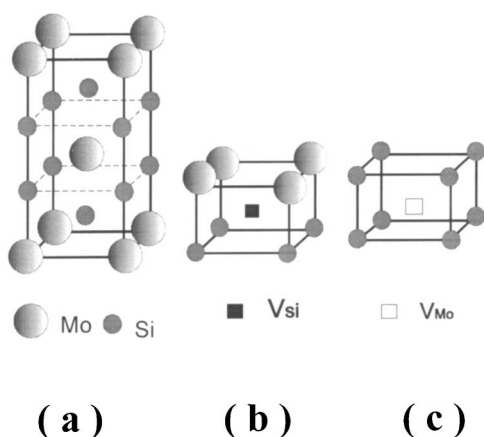


FIG. 4. Perfect and defected lattice structures of MoSi_2 : (a) defect-free MoSi_2 , (b) vacancy located on the Si sublattice, (c) vacancy located on the Mo sublattice.

regions ($p_L \geq 20 \times 10^{-3} m_0 c$) of the Doppler broadened spectra, which are characteristic of high-momentum core electrons, can be made use of for analyzing the chemical nature of the atoms surrounding a vacancy, or in the present case, the sublattice on which the radiation-induced vacancies are located.

In Fig. 3, data of coincident Doppler broadening measurements on MoSi_2 and pure defect-free Mo are plotted after normalization to the data on pure defect-free Si. The data of the Doppler broadened spectra obtained for Mo and Si in the present work are very similar to those obtained by Nagai, Tong, and Hasegawa.²⁵ The chemical surrounding of the positron annihilation site can be specifically characterized by the slope of a Doppler broadening ratio curve in the high-momentum core electron regime. This can be demonstrated by *ab initio* calculations for SiC and vacancies therein.²⁶ The data of defect-free annealed MoSi_2 in the core electron momentum range $(20-30) \times 10^{-3} m_0 c$ exhibit a slope (marked as *a*) quite similar to that of pure Mo (marked as *b*) and entirely different from that of pure Si (horizontal line). This demonstrates that the positron wave function in defect-free MoSi_2 is located predominantly in the vicinity of the Mo sublattice. This behavior may originate from a substantial electron charge transfer from Si to the transition metal Mo similar to the situation in transition-metal aluminides where a significant charge transferring to the transition metal was calculated.²⁷⁻²⁹ This enhances the positron affinity of the Mo sublattice in MoSi_2 in contrast to the pure components, where for Si a higher positron affinity has been reported than for Mo.³⁰

After 0.5-MeV electron irradiation of MoSi_2 , where vacancies are induced exclusively on the Si sublattices, the Doppler broadening spectrum shown in Fig. 3 is still very similar to that of defect-free MoSi_2 . This supports the picture that the vacancies with a positron lifetime of 139 ps induced by 0.5-MeV electron irradiation are located on the Si sublattice and that the positrons trapped there preferentially sample the surrounding Mo atoms.

When the electron energy for irradiation is increased, the

average slope of the ratio curves of the electron momentum distribution in the range of $p_L = (20-30) \times 10^{-3} m_0 c$ of the Doppler broadening spectra, such as *c* and *d*, is changed towards the behavior of pure defect-free Si, which is approached with a nearly horizontal behavior after irradiation with 3-MeV electrons (see the slope *d*). From this change in slope of the core electron momentum distribution after 3-MeV electron irradiation we can directly conclude that the positrons are predominantly annihilated in vacancies with nearest-neighbor Si atoms, i.e., in vacancies on the Mo sublattice (Fig. 4). This confirms the picture that has been anticipated from the positron lifetime data where the longer lifetime of 156 ps has been ascribed to V_{Mo} . The detection of V_{Si} , which are expected to be generated during 3-MeV electron irradiation concomitantly with vacancies on the Mo sublattice, may be suppressed by a reduced specific positron trapping rate and a displacement cross section of Si inferior to that of Mo, in analogy to the displacement cross section of C lower than that of Ta in TaC.¹⁵ The higher displacement cross section of Mo atoms ($\sigma_d = 107 \times 10^{-28} \text{ m}^2$) compared to that of Si atoms ($\sigma_d = 26 \times 10^{-28} \text{ m}^2$)^{14,31,32} leads to a vacancy concentration on the Mo sublattice much higher than that on the Si sublattice in the case of high-energy electron irradiation.

Divacancies of the types $V_{\text{Si-Si}}$ or $V_{\text{Si-Mo}}$ may, in principle, be generated in MoSi_2 during 3-MeV electron irradiation according to the maximum transferred energies E^{col} and the displacement threshold energies T_d of the atoms in MoSi_2 (Table II), whereas the generation of $V_{\text{Mo-Mo}}$ is less likely. However, the near zero slope of the ratio curve of the core-electron momentum distribution in Fig. 3 after 3-MeV irradiation demonstrates that the vacancies are surrounded predominantly by Si atoms, so that in this case predominant single vacancies V_{Mo} on the Mo sublattice are detected. We think that the relatively low value of the positron lifetime (156 ps) additionally favors single vacancies.

Above results and discussions indicate clearly that single vacancies V_{Mo} are predominantly induced in MoSi_2 after 3-MeV electron irradiation.

It should be mentioned here that the decrease of the Doppler broadening intensity at high momenta $p_L = (20-30) \times 10^{-3} m_0 c$ upon vacancy generation by electron irradiation is observed in analogy to the “localization peak” in the ratio curves of pure Al when positrons are trapped at thermally formed vacancies.³³ However, in the present more complex situation of vacancies on the Si or Mo sublattices in MoSi_2 the very different behavior of the slope of the high-momentum Doppler broadening can be specifically employed, together with the data for the pure components, for identifying the sublattices of the vacancies detected here.

IV. CONCLUSIONS

In the intermetallic compound MoSi_2 with favorable high-temperature properties for structural applications, vacancies on the Si sublattice (V_{Si}) and predominantly on the Mo sublattice (V_{Mo}) were selectively introduced by irradiation with electron energies either between the displacement threshold energies of Si and Mo atoms or above these displacement

threshold energies, and were specifically detected by both positron lifetime spectroscopy and coincident Doppler broadening spectroscopy of the positron annihilation, which yields information on the local chemical environment of vacancies.

After 0.5-MeV electron irradiation below the Mo displacement threshold in the MoSi₂ the radiation-induced vacancies characterized by a 139 ps positron lifetime are located on the Si sublattice (V_{Si}). After 3-MeV electron irradiation, the positrons are predominantly trapped by vacancies with a positron lifetime of 156 ps and a Si rich sur-

rounding as characteristic for vacancies on the Mo sublattice (V_{Mo}).

ACKNOWLEDGMENTS

X.Y.Z. thanks the Alexander von Humboldt Foundation for financial support. We are indebted to Professor U. Kneissl for his cooperation in the DYNAMITRON experiments, to L. Raschke for his help during the electron irradiation experiments, and W. Maisch and H. Wendel for specimen preparation.

*Corresponding author: College of Materials Science and Engineering, Yanshan University, Hebei street 438, Qinhuangdao 066004, P. R. China. Electronic address: xiangyi@itap.physik.uni-stuttgart.de; xyzh66@yahoo.com.cn

¹K. Ito, T. Yano, T. Nakamoto, M. Moriwaki, H. Inui, and M. Yamaguchi, Prog. Mater. Sci. **42**, 193 (1997).

²S. A. Maloy, T. E. Mitchell, and A. H. Heuer, Acta Metall. Mater. **43**, 657 (1995).

³H.-E. Schaefer, B. Damson, M. Weller, E. Arzt, and E. P. George, Phys. Status Solidi A **160**, 531 (1997).

⁴E. P. George and I. Baker, Intermetallics **6**, 759 (1998).

⁵H.-E. Schaefer and K. Badura-Gergen, Defect Diffus. Forum **143–147**, 193 (1997).

⁶H.-E. Schaefer, K. Frenner, and R. Würschum, Phys. Rev. Lett. **82**, 948 (1999).

⁷P. A. Kumar, M. Alatalo, V. J. Ghosh, A. C. Kruseman, B. Nielsen, and K. G. Lynn, Phys. Rev. Lett. **77**, 2097 (1996).

⁸K. Saarinen, T. Laine, K. Skog, J. Mäkinen, and P. Hautojärvi, Phys. Rev. Lett. **77**, 3407 (1996).

⁹H. Inui, K. Ishikawa, and M. Yamaguchi, Intermetallics **8**, 1131 (2000).

¹⁰H.-E. Schaefer, Phys. Status Solidi A **102**, 47 (1987).

¹¹K. Matsuda, Y. Shirai, and M. Yamaguchi, Intermetallics **6**, 395 (1998).

¹²J. W. Corbett and J. C. Bourgoin, in *Point Defects in Solids*, edited by J. H. Crawford and L. M. Slifkin (Plenum, New York, 1975), p. 137.

¹³A. L. Barry, B. Lehmann, D. Fritsch, and D. Bräunig, IEEE Trans. Nucl. Sci. **38**, 1111 (1991).

¹⁴H. Inui, H. Mori, and H. Fujita, Philos. Mag. B **61**, 107 (1990).

¹⁵D. Gosset, J. Morillo, C. Allison, and C. H. de Novion, Radiat. Eff. Defects Solids **118**, 207 (1991).

¹⁶C. Y. Allison, R. E. Stoller, and E. A. Kenik, J. Appl. Phys. **63**, 1740 (1988).

¹⁷F. Rullier-Albenque and J. P. Senateur, Radiat. Eff. **88**, 17 (1986).

¹⁸F. Rullier-Albenque and Y. Quere, Phys. Lett. **81A**, 232 (1981).

¹⁹D. Lesueur, J. Morillo, H. Mutka, A. Audouard, and J. C. Jousset, Radiat. Eff. **77**, 125 (1983).

²⁰M. Alatalo, H. Kauppinen, K. Saarinen, M. J. Puska, J. Mäkinen, P. Hautojärvi, and R. M. Nieminen, Phys. Rev. B **51**, 4176 (1995).

²¹T. Laine, K. Saarinen, J. Mäkinen, P. Hautojärvi, C. Corbel, L. N. Pfeiffer, and P. H. Citrin, Phys. Rev. B **54**, R11 050 (1996).

²²M. A. Müller, A. A. Rempel, K. Reichle, W. Sprengel, J. Major, and H.-E. Schaefer, Mater. Sci. Forum **363–365**, 70 (2001).

²³M. A. Müller, W. Sprengel, J. Major, and H.-E. Schaefer, Mater. Sci. Forum **363–365**, 85 (2001).

²⁴Y. Nagai, M. Hasegawa, Z. Tang, A. Hempel, K. Yubuta, T. Shimamura, Y. Kawazoe, A. Kawai, and F. Kano, Phys. Rev. B **61**, 6574 (2000).

²⁵Y. Nagai, Z. Tang, and M. Hasegawa, Radiat. Phys. Chem. **58**, 737 (2000).

²⁶T. E. M. Staab, L. M. Torpo, M. J. Puska, and R. M. Nieminen, Mater. Sci. Forum **353–356**, 533 (2001).

²⁷M. Sob, H.-E. Schaefer, and R. Würschum, Acta Universitatis Wratislaviensis No. 1342, Matematika, Fizyka, Astronomia LIX, 161 (1991).

²⁸J. Xu, B. I. Min, A. J. Freeman, and T. Oguchi, Phys. Rev. B **41**, 5010 (1990).

²⁹C. Müller, H. Wonn, W. Blau, P. Ziesche, and V. P. Kriutskii, Phys. Status Solidi B **95**, 215 (1979).

³⁰M. J. Puska, P. Lanki, and R. M. Nieminen, J. Phys.: Condens. Matter **1**, 6081 (1989).

³¹P. Ehrhart, P. Jung, H. Schultz, and H. Ullmaier, in *Numerical Data and Functional Relationships in Science and Technology*, edited by O. Madelung, Landolt-Börnstein Group II, Vol. 25 (Springer-Verlag, Berlin, 1991), p. 8.

³²D. Lesueur, J. Morillo, and H. Mutka, Radiat. Eff. **77**, 125 (1983).

³³K. G. Lynn, J. E. Dickman, W. L. Brown, M. F. Robbins, and E. Bonderup, Phys. Rev. B **20**, 3566 (1979).

³⁴R. Würschum, K. Badura-Gergen, E. A. Kümmerle, C. Grupp, and H.-E. Schaefer, Phys. Rev. B **54**, 849 (1996).